Bulgarian Chemical Communications, Volume 45, Special Issue A (pp. 211 – 218) 2013

Novel materials as oxygen carriers for energy applications

A. Evdou[1,2], V. Zaspalis[1,2], L. Nalbandian[1]*

[1]*Laboratory of Inorganic Materials (LIM), Chemical Process & Energy Resources Institute, Center for Research and Technology - Hellas (CPERI / CERTH), P.O. Box 60361, 57001, Thermi-Thessaloniki, Greece,*
[2]*Department of Chemical Engineering, Aristotle University, PO. Box 1517, 54006, Thessaloniki, Greece*

Received May 27, 2013; Revised August 18, 2013

Perovskites have the ability to accommodate large concentrations of vacancies in their structure and to reversibly pick up and deliver oxygen at high temperatures, thus they are ideal candidates for use as oxygen carrier materials. The performance of perovskites with the general formula $La_{1-x}Me_xM_yFe_{1-y}O_3$ (Me = Sr, Ca, M = Ni, Co, Cr, Cu) as both oxygen carriers for syngas generation from methane in the Chemical Looping Reforming (CLR) concept and as dense membrane materials in the Dense Membrane Reactor (DMR) concept is explored in the present work. Oxygen is withdrawn from the crystal lattice of the perovskites by oxidation of a fuel. Water, oxygen or carbon dioxide, are then added to the solid which provide the necessary oxygen atoms to fill-in the lattice vacancies. The performance of the mixed perovskitic materials doped with 5% M in the B-site (M=Ni, Co, Cr or Cu), is compared. Also, substitution of Sr with Ca in the A-site of the perovskite is explored. Dense, disc shaped membranes of the materials were utilized in a membrane reactor. Experiments at 1000°C revealed the possibility of performing the reduction and oxidation steps simultaneously and isothermally on each side of the membrane reactor. The system is able to operate on partial pressure based desorption without the need of a carbon containing reductant, so that a process towards hydrogen production, based only on renewable hydrogen source such as water, can be established.

Key words: Hydrogen, Perovskites, Chemical-looping reforming, Dense membrane reactor

INTRODUCTION

It has been established that CO_2 emissions resulting from human activity have led to an increase in the atmospheric CO2 concentration, from a pre-industrial level of 280 to 450ppm [1]. This results in a mean annual temperature increase at the earth's surface which is commonly known as global warming.

The optimum approach to minimize CO_2 emissions is to enhance the use of renewable energy resources, such as biomass, solar and wind energies. However, in the medium-term, other ways to reduce CO_2 emissions are receiving increasing interest.

A possible solution is CO_2 sequestration which consists of capturing CO_2 in an emission source and storing it where it is prevented from reaching the atmosphere. [2]. There are currently a number of available processes for CO_2 capture. Increasing interest among them is being gained in the recent years by the Chemical Looping Combustion (CLC) technology [3]. CLC involves the use of a metal oxide as an oxygen carrier. This process is configured with two interconnected fluidized bed reactors: an air reactor and a fuel reactor. The solid oxygen carrier is circulated between the air and fuel reactors. In CLC, the gaseous fuel is fed into the fuel reactor where it is completely oxidized by the lattice oxygen of the metal oxide to CO_2 and water vapor. By condensing water vapour the free-of-water CO_2 can be sequestrated or/and used for other applications. The technology has recently been successfully demonstrated for more than 1000 h and at scales up to 140 kW [4-6].

An alternative promising option to reduce the CO_2 emissions is the use of H_2 as fuel. Presently, hydrogen is produced mostly by reforming of natural gas (i.e. methane), partial oxidation of heavy oils and naphtha and gasification of coal [7-8]. However, in the conventional process, air is used for the oxidation of methane, thus the generation of NO_x is inevitable. Furthermore, the N_2 in the product dilutes the produced syngas and brings about severe purification demands. A promising new procedure for H_2 production from natural gas is the “Chemical Looping Reforming (CLR)” process [9]. In CLR a suitable oxide catalyst is circulated between two reactors as in CLC. In the first reactor methane is oxidized to synthesis gas by the lattice oxygen of the oxide, and in the second reactor, the reduced oxide is re-oxidized by air. This way the products are not diluted with N_2. A schematic diagram of the CLR and/or the CLC process is presented in Figure 1a.

---

* To whom all correspondence should be sent:
E-mail: nalbanti@cperi.certh.gr

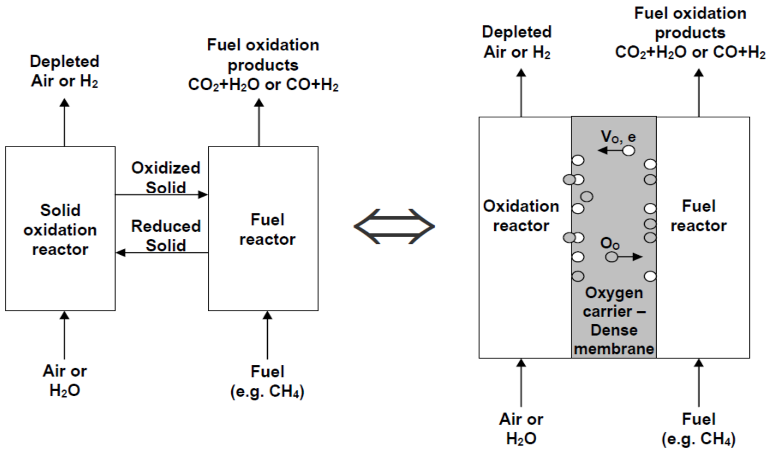

a) b)

Fig. 1. (a) Schematic diagram of the Chemical Looping Combustion (CLC) and/or the Chemical Looping Reforming (CLR) process (b) Dense Membrane Reactor-Chemical Looping Combustion (DMR-CLC) and/or Dense Membrane Reactor-Chemical Looping Reforming (DMR-CLR).

Chemical Looping -Dense Membrane Reactor Concept

One of the biggest concerns in Chemical Looping processes generally and of the CLR specifically is the recirculation of the solid materials between the two reactors. Many materials with good oxygen transfer capacity are not suitable due to their high attrition indices. Furthermore all this movement of solids requires a lot of energy.

In order to overcome these problems the dense membrane reactor concept (Figure 1b) is proposed in this work. It is based on the use of a dense mixed conducting membrane reactor to perform the reduction and oxidation steps simultaneously at either membrane side. It is composed of two compartments gas tightly separated by the dense membrane. A hydrocarbon (e.g. natural gas) is oxidized in the "Fuel" compartment in the absence of gaseous oxygen, by pulling oxygen atoms from the solid. Due to chemical potential difference, oxygen is transferred through the membrane from the opposite "oxidation" side. If air is added in the "oxidation" compartment, gaseous oxygen molecules decompose on the membrane surface and the oxygen atoms fill the oxygen vacancies of the membrane. Alternatively, water can be added in this compartment, which decomposes on the membrane surface into oxygen atoms that fill the oxygen vacancies and pure gaseous hydrogen, ready to use in fuel cell applications.

In either case, a net oxygen flow is formed in the dense membrane from the "oxidation" side to the "fuel" side, which renews continuously the oxygen content of the oxygen carrier, thus permitting the uninterrupted oxidation of the fuel. At the same time, a counter flow of oxygen vacancies (Vo) is formed from the "fuel" side to the "oxidation" side of the membrane, thus permitting the uninterrupted consumption of oxygen.

The dense membrane reactor (Figure 1b) is compared to the general scheme of the chemical looping processes (Figure 1a). The general scheme of the 2 processes is very much alike. They both have a "fuel reactor" in which the fuel is oxidized in the absence of gaseous oxygen, by utilizing the lattice oxygen of a solid "oxygen carrier (OC)". They also both have an "oxidation reactor" where the solid OC is refilled with oxygen, by either air or H_2O. In the Chemical Looping the OC is a powdered solid while in the dense membrane reactor the OC is the membrane itself. Thus the two processes are equivalent and readily interchangeable. The advantage of the dense membrane reactor process is that it ensures continuous and isothermal operation of the Chemical Looping Processes, while there is no need for energy demanding solid recirculation.

One key issue with the Dense Membrane Reactor - Chemical Looping Reforming (DMR-CLR) process that needs to be further studied is the development of the proper materials that can serve as both oxygen carriers and oxygen ion conducting membranes. The ideal candidate materials should:

- be able to accommodate large concentrations of vacancies in their structure
- be able to reversibly pick up and deliver oxygen at high temperatures
- have high catalytic activity in methane partial oxidation

- have good thermal stability and suitable mechanical properties
- exhibit mixed type conductivity for the necessary transfer of anions, vacancies and electrons

Perovskite-type mixed conducting materials are ideal candidates for use in Dense Membrane Reactor - Chemical Looping Reforming, since they fulfil most of the above characteristics.

The performance of the candidate materials is ranked by taking into account the H_2 and CO yields during the fuel oxidation step as well as the amount of oxygen per mole solid (δ) that can be delivered reversibly to the fuel.

EXPERIMENTAL

Powder material synthesis and membrane preparation

The metal precursors used were: $La(NO_3)_2 \cdot 6H_2O$ (Fluka Analytical), $Sr(NO_3)_2$ (Sigma Aldrich), $Fe(NO_3)_3 \cdot 9H_2O$ (Merck), $Ni(NO_3)_2 \cdot 6H_2O$ (Merck), $Co(NO_3)_2 \cdot 6H_2O$ (Sigma Aldrich), $Cr(NO_3)_3 \cdot 9H_2O$ (Merck) and $Cu(NO_3)_2 \cdot 3H_2O$ (Merck). High purity Black Nickel Oxide (NiO) (Ni content 76.6-77.9%) was purchased from Inco Special Products. Anhydrous citric acid (purity >99.5%) was purchased from Sigma Aldrich.

Materials are synthesized by the citrate method [10]. Stoichiometric amounts of the precursors of the corresponding metals are dissolved in deionised water. After the addition of an aqueous citric acid solution, 10% in excess, the solution is stirred, evaporated at 70°C and the obtained solid is dried at 250°C, overnight. Finally the solids are calcined at 1000°C, in air, for 6 h.

The dried powdered sample was initially ball-milled, dried, roll-granulated and uniaxially pressed in the form of cylindrical pellets with a diameter of 10mm and height 15mm. The compacted speciments were sintered in air and cut in thin slices, thickness 1–5mm, with a diamond micro wheel (Struers, Accutom-5).

Material characterization

The basic physicochemical characterization of the prepared samples includes crystalline phase identification, surface area determination and morphology observation by Scanning Electron Microscopy. The crystalline phases formed in the prepared samples are examined by X-ray diffraction. Powder XRD patterns are recorded with a Siemens D500 X-ray diffractometer, with auto divergent slit and graphite monochromator using CuKα radiation, having a scanning speed of 2° min^{-1}. The characteristic reflection peaks (d-values) are matched with JCPDS data files and the crystalline phases are identified. Specific surface area, pore volume and pore size distribution are determined by Nitrogen adsorption – desorption isotherms at the boiling point of liquid nitrogen (77 K) under atmospheric pressure using a Micromeritics, Tristar instrument. Prior to N_2 sorption measurements, the samples are degassed at 523 K, under vacuum, for at least 16 hours. A JEOL 6300 instrument equipped with Oxford – ISIS EDS was used for the morphology observation of the samples.

Pulse reaction experiments

The capability of the prepared powders to deliver oxygen at high temperatures and to convert CH_4 to synthesis gas during the fuel oxidation step, as well as their ability to reversibly pick up oxygen during the solid oxidation step are evaluated by pulse reaction experiments in a fixed bed pulse reactor. Reaction experiments with the materials in powder form are performed in a reaction unit (Altamira AMI-1) using a U-type quartz reactor into which 100±3 mg catalyst is inserted (Figure 2). A detailed description of the experimental unit is provided elsewhere [11-12]. During the fuel oxidation step, methane is fed to the reactor as constant volume pulses, through a special closed loop valve, in pulses of volume 100μl. During the catalyst oxidation step, either oxygen or water is injected to the reactor, also as constant volume pulses, at its entrance before the catalyst. The reactor outlet stream is directed to a quadrupole mass spectrometer (Baltzers – Omnistar) where all the reaction products are continuously monitored and quantitatively analyzed, based on calibration curves for all reactants and products of the process.

Membrane reactor experiments

The membrane reactor consists of two co-axial tubes as shown in Figure 3. The membrane specimen is fixed on top of the inner α-Al_2O_3 tube and divides the membrane reactor into two compartments. An inlet and an outlet stream exist in each compartment, all connected individually to a mass spectrometer (Balzers-Omnistar) for chemical analysis. The membrane specimen is gas tightly sealed at the end of the inner tube with specially developed ceramic sealing mixtures based on commercially available ceramic kits. To control leakage free operation during the entire duration of the experiment, different inert carrier gases are used; helium is used in compartment 1 and argon in compartment 2.

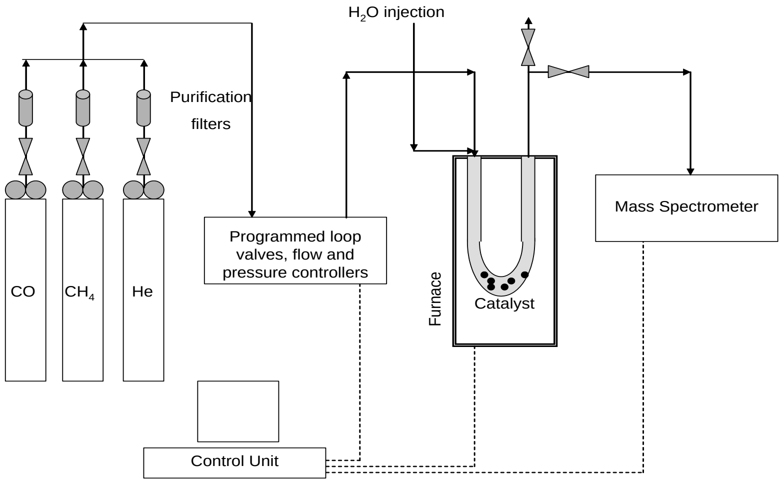

Fig. 2. Schematic flow diagram of the experimental setup used for the reaction experiments

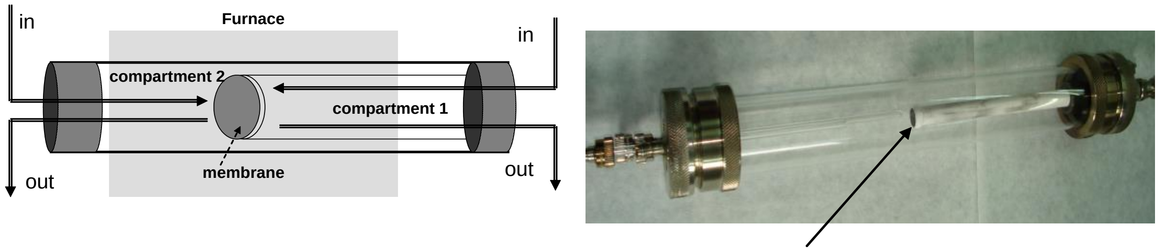

Fig. 3. Schematic diagram (left) and image (right) of the laboratory constructed membrane reactor

RESULTS AND DISCUSSION

Physicochemical characterization

The prepared $La_{0.7}Sr_{0.3}M_{0.05}Fe_{0.95}O_3$, samples for M=Ni, Co, Cr and Cu, are examined by X-ray diffraction in order to identify the crystalline phases formed. All the samples are crystallized in mixed perovskitic structures similar to the mixed compound $La_{1-x}Sr_xFeO_3$ (JCPDS card 35-1480) which is the major phase identified in the $La_{0.7}Sr_{0.3}FeO_3$ sample. No impurities or unreacted species are identified in the XRD patterns of the prepared powders with 5% substitution of Fe, indicating that the second metal (M) is in all cases incorporated in the perovskitic structure.

The surface area of all the synthesized powders is relatively small (< 5 m^2/g), as they are prepared by calcination at high temperatures (1000°C).

Pulse reaction experiments

Experimental procedure: The capability of all the prepared powders to reversibly deliver and pick up oxygen was evaluated by successive reduction – oxidation steps in the fixed bed reactor. During the reduction – fuel oxidation step, CH_4 was used as the reductant, in all experiments. During the solid oxidation step air, water or carbon dioxide injections were used.

A typical plot of the amount of oxygen exchanged by the perovskite sample during three different experiments is shown in Figure 4a. Both experiments start with 25 constant volume (100 μl) injections of CH_4. During the CH_4 injections step, the solid is delivering its lattice oxygen to the fuel, according to the reactions (1) and (2):

$$La_{1-x}Sr_xM_yFe_{1-y}O_3 + \delta_1/4\ CH_4 \rightarrow \delta_1/4\ CO_2 + \delta_1/2\ H_2O + La_{1-x}Sr_xM_yFe_{1-y}O_{3-\delta1} \quad (1)$$

$$La_{1-x}Sr_xM_yFe_{1-y}O_3 + \delta_2\ CH_4 \rightarrow \delta_2\ CO + 2\ \delta_2\ H_2 + La_{1-x}Sr_xM_yFe_{1-y}O_{3-\delta2} \quad (2)$$

thus becoming oxygen deficient.

In the first experiment air, as constant volume pulses, is injected to the reactor, in order to oxidize the solid. During the oxidation step, the solid is recovering its oxygen stoichiometry, according to the reaction (3):

$$La_{1-x}Sr_xM_yFe_{1-y}O_{3-\delta} + O_2 \rightarrow La_{1-x}Sr_xM_yFe_{1-y}O_3 \quad (3)$$

reaching its initial, fully oxidised state.

In the second experiment, the 25 methane pulses are followed by water injections. The solid in this case splits water in order to replenish its lattice oxygen, while producing H_2.

$$La_{1-x}Sr_xM_yFe_{1-y}O_{3-\delta}+H_2O \rightarrow H_2+La_{1-x}Sr_xM_yFe_{1-y}O_3 \quad (4)$$

In the third experiment carbon dioxide is injected to the reactor, in order to oxidize the solid. In this case carbon monoxide is produced, according to reaction (5).

$$La_{1-x}Sr_xM_yFe_{1-y}O_{3-\delta}+CO_2 \rightarrow CO+La_{1-x}Sr_xM_yFe_{1-y}O_3 \qquad (5)$$

As shown in Figure 4a, the final state reached by the solid in the 2 later cases is not the fully oxidised state, as with the O_2 injections. This is due to the different Gibbs free energies of the 2 oxidation reactions of the B-cation ($Fe^{2+} \rightarrow Fe^{3+}$ and $Fe^{3+} \rightarrow Fe^{4+}$), required in order the perovskite to reach its initial oxidation state, as has been discussed elsewhere [13].

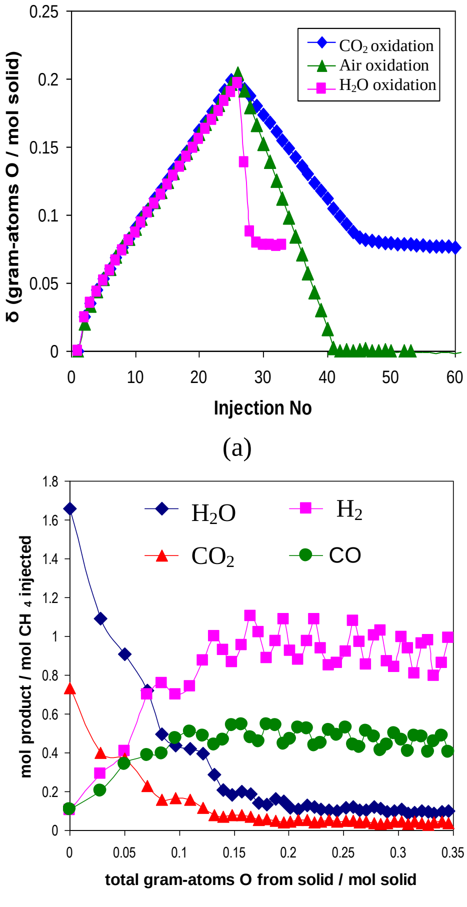

(a)

(b)

Fig. 4. Sample $La_{0.7}Sr_{0.3}FeO_3$ (a) Oxygen loss and uptake (b) product distribution during the fuel oxidation step

A typical product distribution during the fuel oxidation step is shown in Figure 4b. Initially, at low δ, only H_2O and CO_2 are produced. At higher oxygen deficiency of the solid, the yields of water and carbon dioxide decrease and finally only H_2 and CO are produced. As shown in Figure 4b, the product yields are almost stable in a wide range of δ values.

<u>Effect of a second metal addition in the B-position</u>: The performance in the fuel oxidation and the solid oxidation reactions was studied initially for the “reference case” sample $La_{0.7}Sr_{0.3}FeO_3$ with no substitution in the B-position (y=0).

The mixed perovskites with the general formula $La_{0.7}Sr_{0.3}M_yFe_{1-y}O_3$ (M=Ni, Co, Cu and Cr) are tested at the pulse reactor. Their capability to reversibly exchange oxygen, the product yields during the fuel oxidation step as well as hydrogen production during oxidation with water are compared to each other and to the “reference case” $La_{0.7}Sr_{0.3}FeO_3$ (y=0) material.

In Figure 5 the performance of the mixed perovskite materials doped with 5% M (M=Ni, Co, Cr or Cu), are compared.

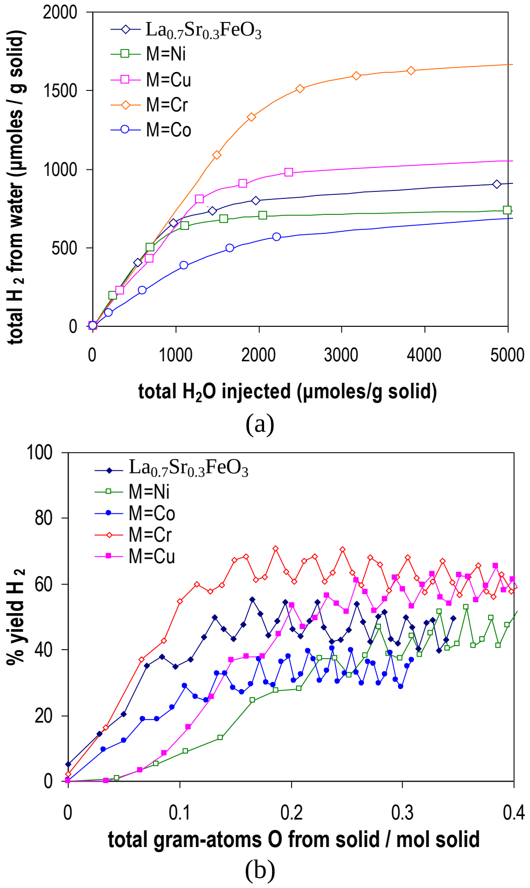

(a)

(b)

Fig. 5. Effect of B-site doping of the $La_{0.7}Sr_{0.3}FeO_3$ perovskite with 5% Ni, Co, Cr and Cu

The H_2 yields obtained with the above samples are compared to the reference sample $La_{0.7}Sr_{0.3}FeO_3$ in Figure 5b. The fully oxidized samples (δ close to 0) present negligible H_2 production. The measured H_2 yields increase with increasing oxygen deficiency of the solid, for all tested samples, until they reach an almost equilibrium value when the oxygen deficiency of the solid exceeds a minimum δ value. Cr and Cu doping increase the obtained H_2

yields compared to the reference case, Ni doping has almost no effect and Co doping has a negative effect, decreasing the obtained H_2 yields during the fuel oxidation step.

In Figure 5a the hydrogen production capability of the prepared 5% doped perovskites, when water is injected instead of air during the solid oxidation step, is compared to the corresponding H_2 production capability of the "reference case" $La_{0.7}Sr_{0.3}FeO_3$ perovskite.

In Figure 5a, the total quantity of produced H_2 is shown as a function of the quantity of injected H_2O. The total quantity of produced hydrogen with the Cu and Cr doped perovskites is higher than the "reference case", while total H_2 with the Ni and Co doped samples is lower. Doping with Cr gives the best hydrogen production capability, among the perovskites prepared in this study.

By combining the results shown in Figure 5 it can be concluded that the Cr doped sample gives the best performance, both in the fuel oxidation step where it has the highest H_2 yield and in water splitting during the oxidation step where it produces the highest H_2 quantities.

Effect of a second metal addition in the A-position: In order to study the effect of replacing the metal at the A site of the perovskite, Sr was replaced by Ca. The performance of the perovskites with the general formula $La_{1-x}Ca_xFeO_3$ (x=0.3, 0.5, 0.7) is compared to the "reference case" $La_{0.7}Sr_{0.3}FeO_3$ in Figure 6.

From Figure 6a, where the H_2 yield during the fuel oxidation step is shown, it can be observed that for all the Ca containing perovskites the maximum H_2 yields are identical to the "reference case" sample. However, the production of the desired products, H_2 and CO in the presence of all $La_{1-x}Ca_xFeO_3$ samples, reaches its maximum at significantly lower oxygen non-stoichiometry values (δ). In Figure 6b the water splitting capability of the $La_{1-x}Ca_xFeO_3$ materials, during the solid oxidation step, as percent H_2O conversion, is compared to that of the "reference case" perovskite. It can be observed that for all the Ca containing samples, oxidation with water proceeds until much lower O-nonstoichiometry (δ) values, compared to the reference case perovskite. Furthermore, the final δ value becomes lower as the Ca/La ratio of the perovskite decreases.

Membrane reactor experiments

In the membrane reactor the two steps of the water splitting reaction, lattice oxygen removal-activation and hydrogen production–deactivation, are performed simultaneously at the different compartments of the reactor.

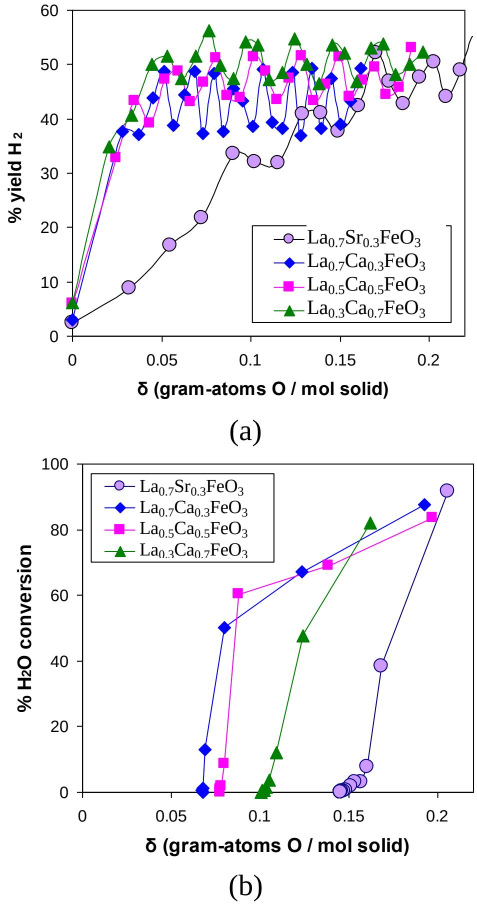

Fig. 6. Effect of A-site doping of the $La_{1-x}Me_xFeO_3$ perovskite with Sr or Ca

Membrane specimens of the composition $La_{0.7}Sr_{0.3}FeO_3$ are mounted in and tested at the membrane reactor. Because of technical reasons related with the complexity of mass spectrometry analysis, the experiments towards demonstrating the membrane reactor principle are performed with carbon monoxide as the reductant at the activation step, instead of methane which was used during the batch reactor experiments.

During a typical experiment, the membrane reactor is heated to 860°C, initially with inert gas flow in both compartments, while the signals of water and hydrogen in compartment 1 are continuously monitored. The injection of water in compartment 1 does not involve any changes in the signal of hydrogen in compartment 1, which maintains its background value, since the membrane is initially inactive.

The injection of CO in compartment 2, results in the reduction of the membrane surface in side 2, creating oxygen vacancies. Due to the ionic conductivity of the perovskitic material the oxygen vacancies are transported through the crystal lattice to the surface of the membrane in compartment 1 and activate it. The water that is injected in compartment 1 is thus split, hydrogen is produced, while simultaneously oxygen is delivered to the solid which fills its anion vacancies. The lattice oxygen is transported once again via the material to the surface of membrane in compartment 2, where it is continuously consumed oxidising CO. Globally a clean flow of oxygen ions, originating from water, is created, from side 2 to side 1 of the membrane, while simultaneously oxygen vacancies flow from side 1 to side 2 of the membrane. Thus a steady state is reached where the surface of the membrane in compartment 2 is rich in oxygen, continuously oxidising CO, while the membrane surface in compartment 1 is rich in oxygen vacancies, continuously splitting water at the highest initial conversion. By optimising the process parameters e.g. gas flows, temperature, membrane thickness, it is possible to keep the membrane material at its highest activation state, during the steady state operation of the reactor.

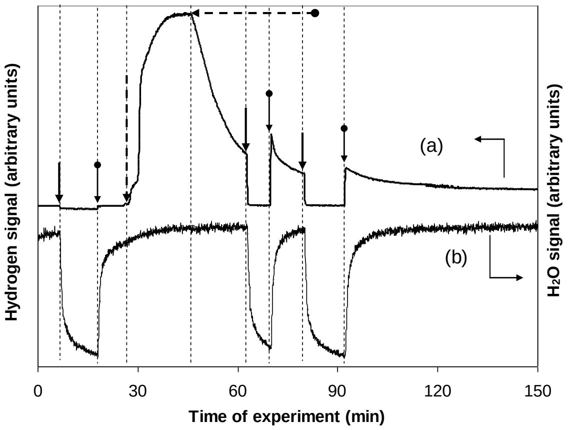

Fig. 7. Hydrogen and water MS signals in compartment 1 during a typical experiment with $La_{0.3}Sr_{0.7}FeO_{3\pm\delta}$ (a) produced H_2 (b) injected H_2O,
⟶: water off, ●⟶ : water on, – –▶: CO on,: ●– –▶CO off

The interruption of CO injection in compartment 2 results in decreased hydrogen production rate in compartment 1. However, hydrogen yield does not become zero, instead it reaches a new steady value, which is of course lower than before (Figure 7). In this case the oxygen ions are desorbed from the membrane surface in side 2 as molecular O_2, only under the effect of oxygen partial pressure difference between the two sides of the membrane. The flow of oxygen ions is in this case smaller, however it is not insignificant. The water continues be split, producing hydrogen which originates only from renewable water.

Periodical water feed shut downs in compartment 1, were performed during this steady state, in order to excluded the possibility of base-line shifting and quantify the obtained results. As shown in Figure 7, interruption of H_2O injection results in a significant drop of the H_2 signal, down to its background value, which proves that the observed hydrogen signal is due to real hydrogen produced from the decomposition of the injected water.

Similar experiments with inactive membrane materials (a-Al_2O_3 and fused silica) did not show any significant change in the hydrogen signal during water feed shut downs, either before or after CO injection in compartment 2.

CONCLUSION

Perovskite materials are suitable for use as oxygen carriers in Chemical Looping Reforming. Upon reduction with methane, powdered $La_{1-x}Sr_xM_yFe_{1-y}O_3$ (M = Ni, Co, Cr, Cu) materials are found to loose oxygen. Subsequent oxidation of the solid is performed either with gaseous oxygen or water or with carbon dioxide. When oxidation takes place with air, heat is generated because the reaction is exothermic. When H_2O is used to oxidize the material, simultaneously is produced very pure H_2, ready to use in fuel cell applications, but the oxidation reaction is endothermic. After oxidation with CO_2, CO produced but again the oxidation reaction is endothermic. The additional heat required during the oxidation with H_2O or CO_2, is the energy penalty for the additional production of H_2 or CO. The best, thus far, performance was obtained with the $La_{0.7}Sr_{0.3}Cr_{0.05}Fe_{0.95}O_3$ sample, with H_2 yield up to 70% and very good stability in repetitive

Acknowledgements: *The present study was funded by the program ''Hydrogen Economy Cooperation Network for Research - Public Awareness - Business Opportunities across Greek-Bulgarian borders – HYDECON''. The Project is co-funded by the European Regional Development Fund and by national funds of the countries participating in the ETCP "Greece-Bulgaria 2007-2013'' through contract B1.33.01.*

REFERENCES

1. Blesl M, Kober T, Bruchof D, Kuder R. *Energy Policy*; **38**, 6278 (2010)
2. ADEME, BRGM, IFP. CO_2 capture and storage in the subsurface. Geoscience Issues, France, 2007.
3. Hossain MM, Lasa HI.. *Chem. Eng. Sci.*, **63**, 4433 (2008)

4. Pröll T, Bolhàr-Nordenkampf J, Kolbitsch P, Hofbauer H. *Fuel*, **89**,1249 (2010)
5. Linderholm C, Mattisson T, Lyngfelt A., *Fuel*, **88**, 2083 (2009)
6. Adánez J, Dueso C, Diego LF, García-Labiano F, Gayán P, Abad A. *Energy & Fuels*; **23,** 130 (2009)
7. Balat M., *Energy Sources Part A*, **31**, 39 (2009)
8. Chen WH, Chiu TW, Hung HI., *Int J Hydrogen Energy*, **35**, 12808 (2010).
9. Diego LF, Ortiz M, Adánez J, García –Labiano F, Abad A, Gayán P., *Chem. Eng. J.*, **144**, 289 (2008)
10. Pecchi G, Reyes P, Zamora R, Campos C, Cadus LE, Barbero BP. *Catal. Today*, **133–135**, 420 (2008)
11. Evdou A, Zaspalis V, Nalbandian L., *Int J Hydrogen Energy*; **33**, 5554 (2008)
12. Evdou A, Nalbandian L, Zaspalis VT., *J Membr Sci.*, **325**, 704 (2008)
13. Nalbandian L, Evdou A, Zaspalis V., *Int J Hydrogen Energy*, **34**, 7162 (2009)

НОВИ МАТЕРИАЛИ КАТО ПРЕНОСИТЕЛИ НА КИСЛОРОД ЗА ЕНЕРГИЙНИ ПРИЛОЖЕНИЯ

А. Евдоу[1,2], В. Заспалис[1, 2], Л. Налбандиан[1]*

[1]*Лаборатория по неорганични материали, Институт по химични процеси и енергийни ресурси,*

Научно-изследователски и технологичен център – Хелас, Терми-Солун, Гърция

[2]*Катедра по химическо инженерство, Аристотелов университет, Солун, Гърция*

Получена на Май 27, 2013; Ревизирана на Август 18, 2013

(Резюме)

Перовскитите имат способността да формират голямо количество ваканции в своите структури и да приемат и отдават обратимо кислород при високи температури, което ги прави идеални кандидати за преносители на кислород. В настоящата разработка е изследвано поведението на перовскити с обща формула $La_{1-x}Me_xM_yFe_{1-y}O_3$ (Me = Sr, Ca, M = Ni, Co, Cr, Cu) като преносители на кислород за генериране на сингаз от метан, както и като плътни мембранни материали. Кислородът се изтегля от кристалната решетка на перовскитите чрез окисление на гориво. След това към твърдата фаза се добавя вода, кислород или въглероден диоксид, което осигурява запълване на ваканциите с необходимите кислородни атоми. Сравнено е поведението на смесени перовскитни материали, заместени с 5% М на В-място (M=Ni, Co, Cr и Cu). Изследвано е също така и заместването на Sr с Ca на А-място в перовскитите. Плътни мембрани от материалите с формата на диск са използвани в мембранен реактор. Проведените експерименти при 1000°C разкриват възможността за едновременно и изотермично провеждане на етапите на редукция и окисление от двете страни на мембранния реактор. Системата може да функционира без добавянето на въглерод-съдържащ редуктор, така че е възможно реализирането на процес за производство на водород, основаващ се на възобновяем водороден източник, напр. вода.